New pathways linking telomeres to cancer formation and progression

77

Pasquale Zizza, Roberto Dinami, Manuela Porru, Eleonora Petti, Erica Salvati, Angela Rizzo, Carmen D'Angelo, Carla Azzurra Amoreo, Marcella Mottolese, Giovanni Blandino, Andrea Sacconi, Carlo Leonetti, **Annamaria Biroccio**.

Department of Research, Diagnosis and Innovative Technologies, IRCCS Regina Elena National Cancer Institute, Rome Italy.

TRF2 is a master regulator of telomere integrity

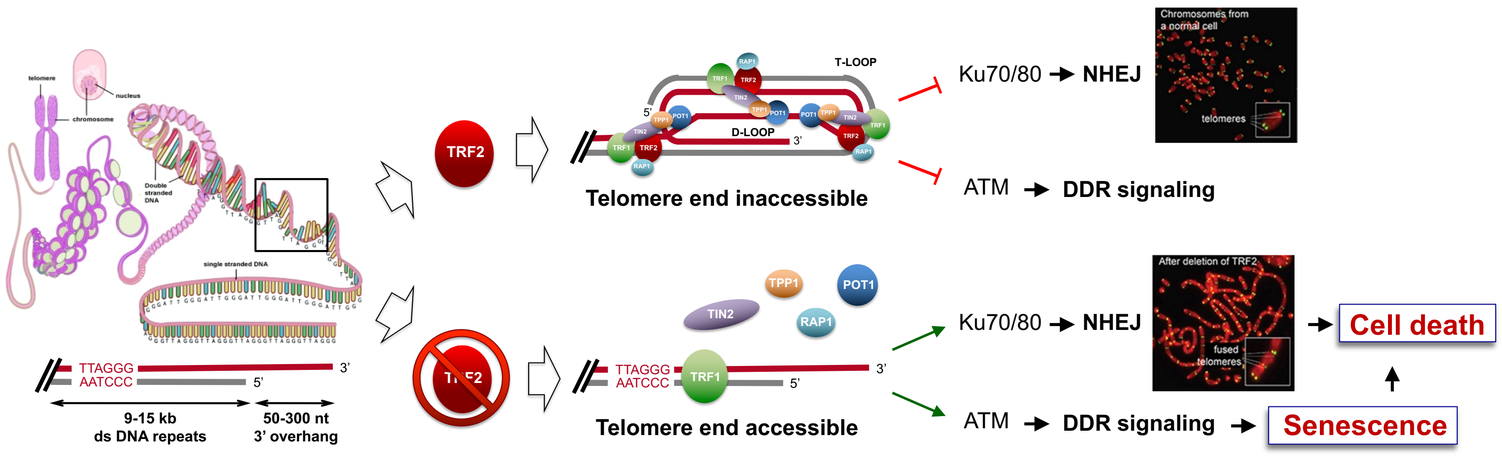

Schematic representation of the main mechanisms through which the telomeric repeat-binding factor 2 (TRF2) maintains telomere integrity. TRF2 binding to telomeric TTAGGG repeated sequences favours assembly of the Shelterin, a multiprotein complex that protects telomere from erosion and inhibits the activation of non-homologous end joining (NHEJ) and DNA damage response. Depletion of TRF2 can determine the activation of those signalling pathways that induce senescence and cell death.

TRF2 is overexpressed in several tumors

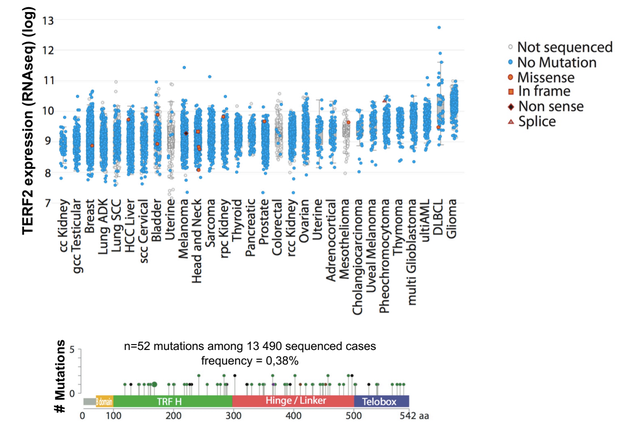

Upper panel - RNAseq analysis of TRF2 expression of 30 tumor histotypes from the cancer genome atlas (TCGA). *Lower panel* - Schematic representation showing numbers, frequencies, and locations of mutations in the TRF2 gene among 13490 sequenced cases.

TRF2 affects gene expression

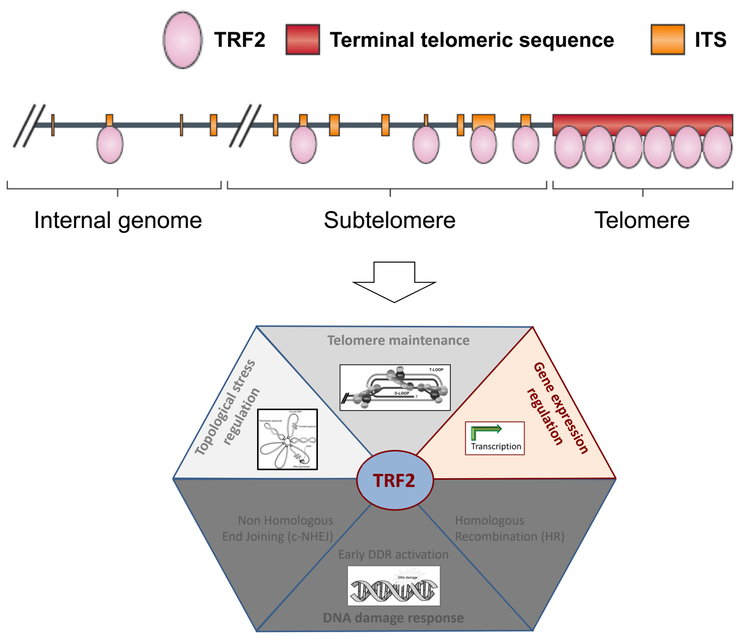

Upper panel – Schematic representation of TRF2 binding sites (telomeric and extratelomeric) on the chromosome. *Lower panel* – Scheme summarizing the main functions of TRF2. Together with the "canonical" telomeric functions we identified a novel extratelomeric function of TRF2 in controlling gene expression.

TRF2 correlates with poor prognosis in CRC

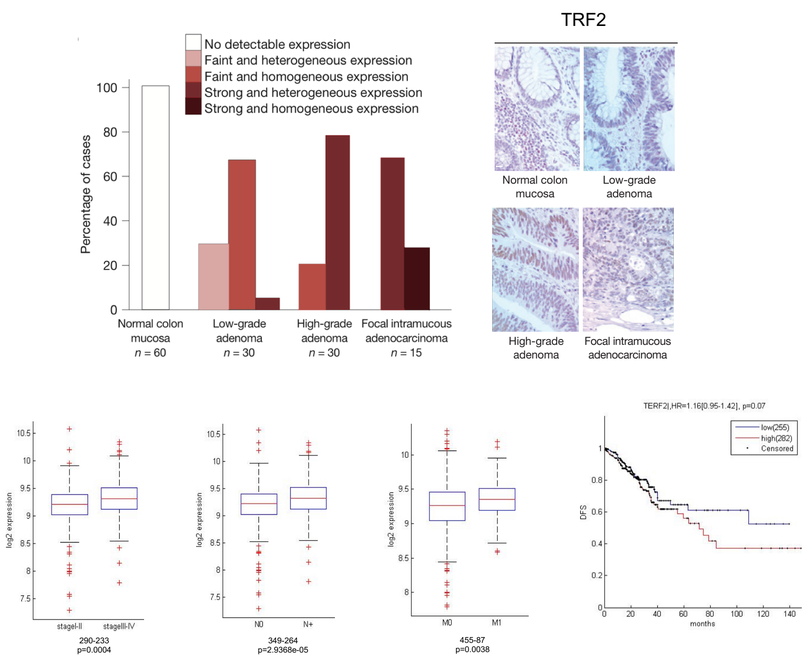

Upper panels – In colorectal cancer (CRC) models, expression of TRF2 positively correlates with progression (TRF2 expression increases moving from normal mucosa to focal intramucous adenocarcinomas). *Lower panels* – A retrospective analysis performed on 537 CRC patients from TCGA revealed that TRF2 expression correlates with tumor stage, lymphnode positivity, metastasis and poor prognosis.

TRF2 silencing does not induce DDR in HCT116 cells

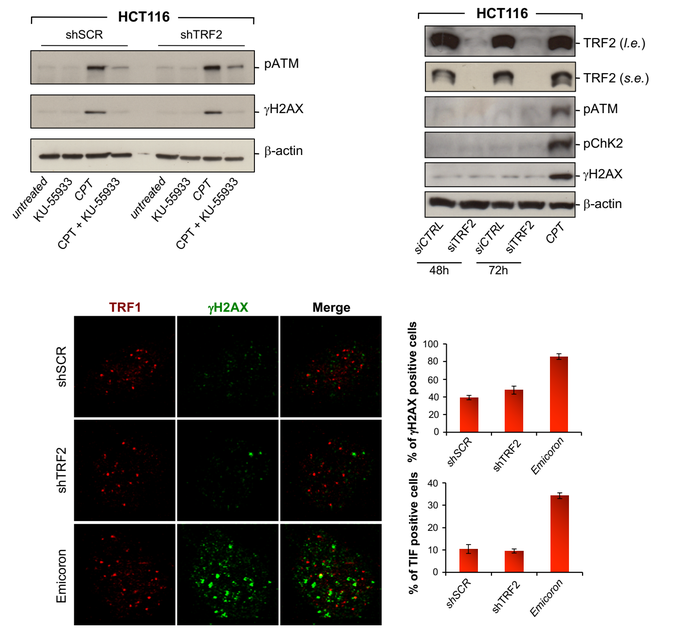

Western blot analysis of damage pathways and immune fluorescence of damage foci were performed in HCT116 cells silenced for TRF2 and their control counterpart. When specified DNA damaging agents Camptothecin (CPT, 0.2 μM for 2h) – in absence or in presence of the ATM inhibitor KU-55933 (5μM, 24h) – or Emicoron (0.5 μM, 24h) were used as controls. HCT116 cells were chosen as experimental model for further studies since it permits to investigate the extratelomeric role of TRF2 without interferences from its telomeric functions.

TRF2 regulates glycocalyx structure of cancer cells and promotes tumor formation and progression by subverting microenvironment

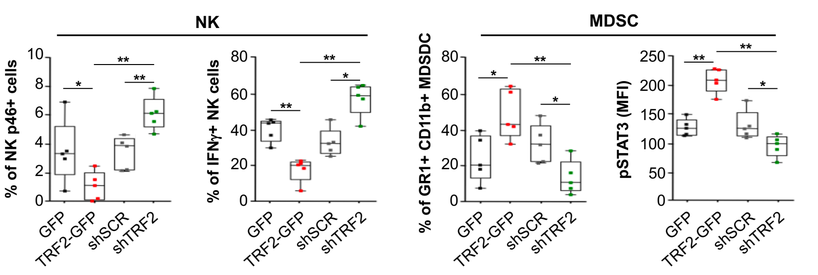

Matrigel-embebbed cells were inoculated into the backs of nude mice (5 mice/group) and after five days the percentage of Matrigel infiltrated (left panels) and activated (right panels) NK cells and MDSCs were evaluated by FACS analysis.

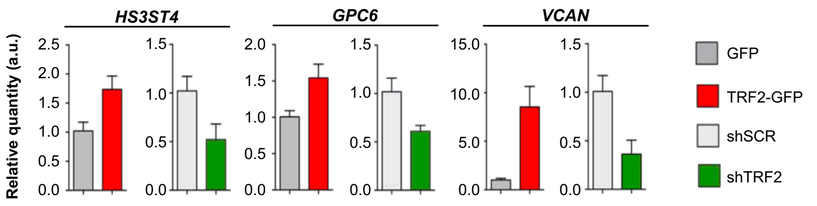

Gene expression analysis by quantitative polymerase chain reaction (qPCR) of TRF2 target genes following TRF2 overexpression or knockdown.

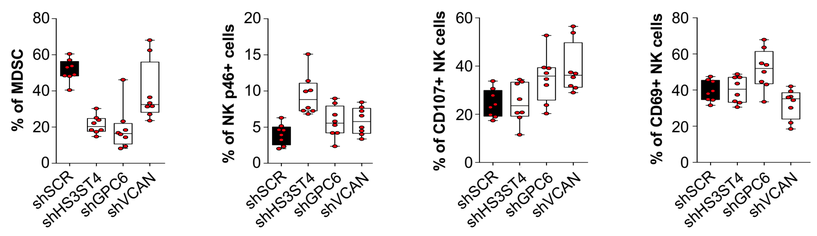

Matrigel-embedded cells stably silenced (sh) for HS3ST4, GPC6 or VCAN or their control counterpart (sh scramble) were inoculated into the back of immunocompromised mice and after 16 days the percentage of MDSC and infiltrating (CD3- NKp46+) or activated (CD107+ or CD69+) natural killer cells in Matrigel plugs was evaluated by FACS analysis.

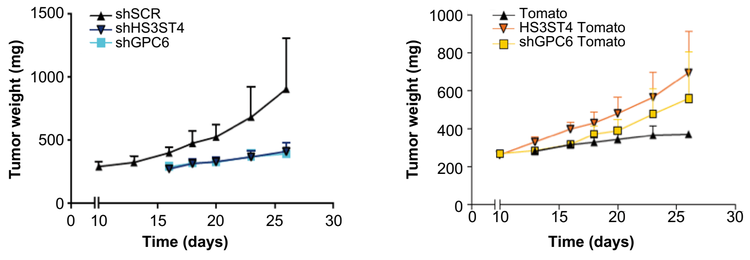

Tumor cells infected as reported in the figure, were subcutaneously injected in immunocompromised mice and tumor weight was evaluated over time after implantation.

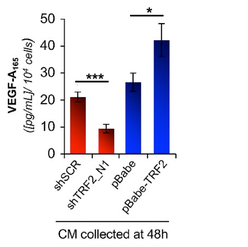

Concentration of VEGF-A_{165} was evaluated by ELISA in the CM of HCT116 silenced or overexpressing TRF2 and their control counterparts. Results were normalized to cell number.

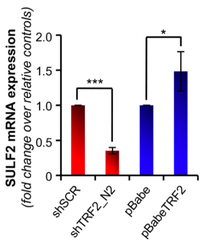

Gene expression of SULF2 was evaluated by qPCR in HCT116 cells silenced or overexpressing TRF2 and in their control counterparts. Results are expressed as fold change of mRNA levels over relative controls, after β-actin normalization.

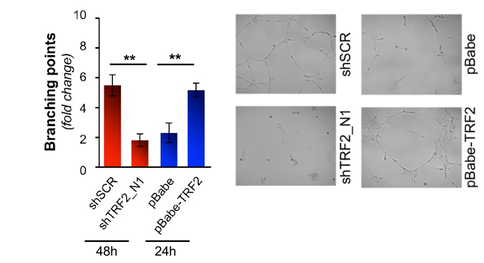

CMs obtained from HCT116 cells silenced or overexpressing TRF2 were collected at the indicated times and their angiogenic potential was evaluated both *in vitro* and *in vivo* by tubule formation assay (*upper panels*) and matrigel assay (*lower panels*), respectively.

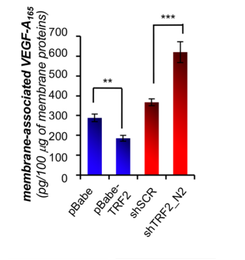

Amount of membrane-associated VEGF-A quantified by ELISA (*upper panel*) performed on membrane-enriched lysate fractions or confocal microscopy (*lower panel*).

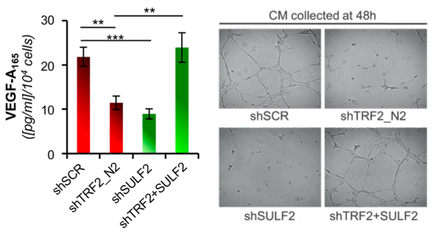

Left panel – Concentration of VEGF-A evaluated by ELISA in the CM of empty vector or SULF2 overexpressing HCT116 cells infected with scramble (shSCR), TRF2 (shTRF2) or SULF2 (shSULF2) targeting shRNAs. Results were normalized to cell number. *Right panel* – The same CMs were assayed for their capability of inducing capillary structures in HUVEC cells. representative images showing tubular-like structures (5X magnification) are shown.

Left panel – Concentration of VEGF-A evaluated by ELISA in the CM obtained from HCT116 cells stably transfected with an empty vector (pBabe) or the vector encoding for TRF2 (pBabe-TRF2) and overexpressing or not SULF2. Results were normalized to cell number . *Right panel* – The same CMs were assayed for their capability of inducing capillary structures in HUVEC cells. representative images showing tubular-like structures (5X magnification) are shown.

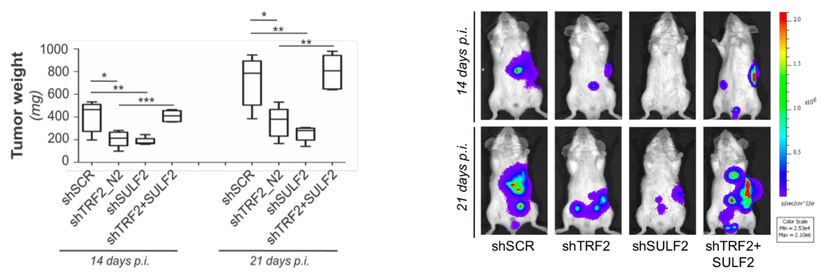

OUR WORK REVEALS HOW TRF2 CHANGES ARE TRANSLATED INTO ONCOGENIC EVENTS LINKED TO CANCER FORMATION AND PROGRESSION, IDENTIFYING A MULTI-HIT TELOMERIC TARGET FOR INNOVATIVE ANTI-CANCER THERAPIES.

Left panel – HCT116 cells, infected as reported in the figure, were intramuscularly injected in immunocompromised nude mice and tumor weight was evaluated by caliper at the indicated days post-injection. The graph shows the mean ±SD from 5 mice per group. *Right panel* – Luminescent HCT116 cells were injected in the spleen of CB17-SCID mice and after 30 min the spleen was removed by spleenectomia. Real-time tumor dissemination was monitored by the IVIS imaging system at the indicated days. Representative images of tumor dissemination are shown.